Fall 2015

A SEM Study Of Copper Corrosion In Bowling Green Supply Lines

Reema M. Alghamdi
Western Kentucky University, reema.alghamdi545@topper.wku.edu

A SEM STUDY OF COPPER CORROSION IN BOWLING GREEN SUPPLY LINES

A Thesis
Presented to
The Faculty of the Department of Chemistry
Western Kentucky University
Bowling Green, Kentucky

In Partial Fulfillment
Of the Requirements for the Degree
Master of Science

By
Reema Alghamdi

December 2015

A SEM STUDY OF COPPER CORROSION IN BOWLING GREEN SUPPLY LINES

Date Recommended 11/10/15

Cathleen J. Webb

Dr. Cathleen Webb,
Director of Thesis

D. Raj

Dr. Rajalingham Dakshinamurthy

Yan Cao

Dr. Yan Cao

12/10/15

Dean, Graduate Studies and Research Date

ACKNOWLEDGEMENTS

I am most grateful to God. I will like to thank my husband for being a great support to me during my challenging moments. My sincere gratitude goes to Dr. Cathleen Webb, my research supervisor. I would also like to thank my committee members Dr. Rajalingam Dakshinamurthy and Dr. Yan Cao. I thank Dr. John Andersland for his help with Scanning Electron Microscopy (SEM). To the members of staff at Advanced Material Institute, I say thank for your help.

TABLE OF CONTENTS

ILLUSTRATION INDEX

INDEX OF TABLES

A SEM STUDY OF COPPER CORROSION IN BOWLING GREEN SUPPLY LINES

Reema Alghamdi December 2015 47 Pages

Directed by: Dr. Cathleen Webb, Dr. Rajalingham Dakshinamurthy, and Dr. Yan Cao

Department of Chemistry Western Kentucky University

Recently, the rate of corrosion of copper water pipes in Bowling Green, Kentucky has unexpectedly accelerated. The specific reasons for this are unknown. Our aim is to elucidate the factors enhancing the corrosion and help understand the primary mechanisms of action. This will help in combating and reducing future corrosion incidents leading to pipe failure, thus reducing losses experienced when these pipes are replaced. This study seeks to explore the characteristics and factors involved. The scanning electron microscopy was used to obtain elemental composition, and images of both inside and outside of the corroded pipes. Strikingly, corrosion primarily occurred on the outside of the pipes, not inside. X-ray crystallography also was used to examine the pipes. The results showed that the interior of the pipes mostly consisted of SiO_2, CuO_2, $CaCO_3$ while the exterior consisted of $Cu_2(OH)_2CO_3$, $Fe_2Al_2O_4$, $CaCO_3$, SiO_2 and Cu_2O. There was no clear single factor for the corrosion observed. For further studies, we plan to long temporal experiments. The results from the study will help in minimizing the costs to the city in Bowling Green, Kentucky.

INTRODUCTION

Natural waters are complex mixtures with many different chemical species in them. The most abundant species are ions. Cations or positively charged ions that are most commonly present are Ca^{2+}, Mg^{2+}, Na^{+} and Fe^{2+}. Anions or negatively charged ions such as HCO^{-}_{3}, CO_3^{2-} , SO_4^{2-} and Cl^{-} are also common. Other species, such as dissolved gases like O_2, CO_2, and sometimes H_2S are present as well. Fresh, with a relatively low ionic strength and sea water, which has a high ionic strength reflect extremes for natural waters. In between, there is a wide variety of water qualities. This variety is also reflected in a sensitivity to metals varies. The most commonly used materials in water distribution pipes are iron, steel, copper, and polyvinyl chloride or PVC. Metals such as iron and copper may experience corrosion problems through reduction-oxidation reactions as well as fouling. The calcium-carbon water balance is important in controlling fouling in distribution networks. These effects can be accelerated by microbial processes (Nawrockia *et al* 2012).

Corrosion of water pipes has severe economic impacts. Countries like Denmark and Sweden have calculated an annual cost of $5.25-5.65 million dollars by corrosion problems in 2013. In the United States, water and sewer municipalities experience $36 billion dollars in corrosion damage annually. In Bowling Green, Kentucky, a household pipeline break costs around $1500 to repair. In recent years, bowling green has experienced 2-3 failures/week, which means more than $100,000 in annual repair costs for the City of Bowling Green. However, given the karst geologic nature, the water loss due to smaller undetected leaks may be high.

In addition, water quality can change and may become distasteful because of alterations in the characteristics of water that pass through the pipes with corrosion. Heavy metals such as cadmium and lead may also be transported readily. For this reason, many countries around the world no longer authorize the use of lead pipes or lead solder (Nawrockia *et al* 2012).

The issue of corrosion in copper water pipes is usually said to be related to the flow rate of water. "The corrosion rate of copper in most drinkable waters is less than 2.5 μm/year. At this rate, a 15 mm tube with a wall thickness of 0.7 mm should last for about 280 years. In some soft waters the general corrosion rate may increase to 12.5 μm/year, but even at this rate it would take over 50 years to perforate the same tube"(Copper pipe Corrosion Copper pipe Corrosion theory and mechanism).

In bowling green, copper pipes are failing due to corrosion after 15 years. Investigation of the related factors for this unexpectedly high failure rate is the motivation for this thesis.

Corrosion Phenomenon

The forms of water pipe corrosion are diverse. The problem is complex because so many factors contribute to it. The most important factors are the flow conditions, the composition of the products and the biological and physicochemical characteristics of water. The presence of water with certain bacterial floras (sulfate-reducing bacteria and

Ferro bacteria) increases corrosion. The chemical characteristic of water influences the presence of bacterial flora and this could accelerate the corrosion (Hamilton, 1985).

Many chloride-containing ground waters are also more corrosive. Chloride comes from many processes such as infiltration of surface water from mining, industrial dumps and seawater intrusion. Concentrations of chloride ions of 1 g per 1iter cause rapid corrosive destruction of metals such as iron and stainless steel. Chloride as low as 100 mg per liter in medium-hard water can also cause corrosion of pipes.

Many chemical species that exist in drinking water affect corrosion of metals differently. High calcium hardness and alkalinity favor the formation of a protective layer of $CaCO_3$ on the water pipes. The presence of certain ions such as chloride and sulfite in concentrations that exceed a certain threshold can radically change the characteristics of the protective layer causing an attack on the base metal (Hamilton, 1985). Different types of corrosion are discussed below.

Bacterial or Microbial corrosion

Microbial corrosion can be defined as a bacterial metabolic process that causes or accelerates the destruction of metals. The role of bacteria in metal corrosion has been known for a long time. Von Wolzogen-Kuhr in 1923 revealed the electrochemical mechanism of iron attacked by microorganisms. Microorganisms are part of the world of unicellular organisms which are widespread throughout the biosphere. They play many important roles in nature such as the decomposition of organic matter. During these biological processes, a variety of end products are formed (Iverson and Warren, 1987).

Microorganisms influence corrosion processes through mechanisms that allow them to acquire the necessary energy for vital activities. This energy can be acquired through three means. The first way is via aerobic respiration which involves the progressive removal of hydrogen from organic substrates. The hydrogen is oxidized by oxygen. The second way is via anaerobic respiration in which the organic substrate is oxidized by hydrogen removal and inorganic compounds are reduced. The third way is via fermentation which is an anaerobic process in which the organic substrate is not completely oxidized. All of these metabolic processes are based on the transfer of hydrogen ions or electrons. The resulting microbial activities are very favorable to corrosion (Iverson, 1987).

Anaerobic Corrosion

Anaerobic corrosion, which was first observed in 1923 in the Netherlands, was caused by *Desulfovibrio*. These bacteria were found to corrode iron and steel by forming ferrous sulfide which resulted in corrosion. Microbial cultures are also strongly reducing systems. The metabolic activity of bacteria is a result of the energy supplied by the oxidation of nutrients that cause reduction conditions. These redox reactions play important roles in biological processes. The electromotive force or potential difference generated by the flow of electrons can be measured. This potential is related to the pH, temperature and the relationship between the concentration of oxidized and reduced substances. Oxidation conditions generally correspond to a high potential while reduction is reflected by a lower potential.

The most common bacteria develop in potential conditions near or below 0 volts and a pH between 6 and 9. The bacteria in these conditions rapidly multiply and metabolize different substances. These processes result in reduced redox potential, creating favorable conditions for electrochemical corrosion (Figure 1). Anaerobic corrosion is considered possible at pH values between 5.5 and 8.5, in which case the value of the redox potential allows for the following classification of corrosion as shown in Table 1.

Table 1. Redox potential and corrosion classification of anaerobic soils containing sulfates.

(Iverson, 1968).

Redox Potential, mV	**Anaerobic corrosion risk**
<100	Severe
100-200	Moderate
200-400	Light
>400	Null

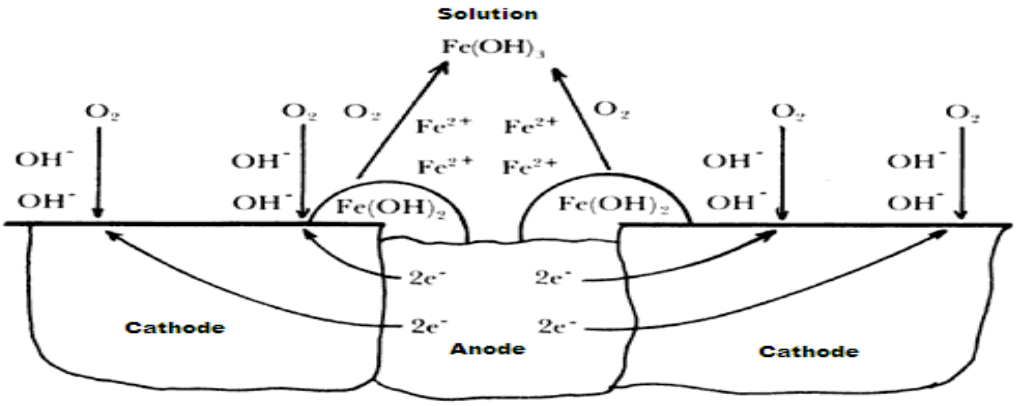

Figure 1: Diagram illustrating the process of electrochemical formation of rust (Iverson, 1968).

Rust is composed of ferric hydroxide, $Fe(OH)_3$. Metallic iron, moisture, and oxygen are required for the corrosion. The corrosion of iron in the presence of oxygen is an electrochemical reaction (Iverson, 1968). Ferrous hydroxide, $Fe(OH)_2$, is formed as a result of ferrous ions Fe^{2+} and hydroxyl ion, OH^-. The negatively charged hydroxyl ions in solution migrate toward the anodic areas where there is an excess of positive charge due to the presence of ferrous ions formed. Ferrous hydroxide is formed when the ferrous ions react with the hydroxide. The ferrous hydroxide is oxidized to ferric hydroxide, $Fe(OH)_3$, by oxygen dissolved in water (Iverson, 1968). The reactions are listed below.

The anodic reaction is Fe □□Fe^{2+} + $2e^-$.

The cathodic reaction is $2H^+ + 2e^-$ □ 2H □□□□□

The ferrous hydroxide is formed: $Fe^{2+} + 2\ OH^-$ □ $Fe(OH)_2$

The overall reaction is $4Fe(OH)_2 + O_2 + 2H_2O$ □ $4Fe(OH)_3$.

Figure 2 shows that the cathodic reaction is the formation area of molecular hydrogen, H_2, on the cathode surface. In neutral solutions, hydrogen formation, and evolution of hydrogen gas are very slow. This is the origin of the formation of hydrogen bubbles on the cathode surface. When this happens, the hydrogen bubble film formed on the cathode may actually decrease the corrosion rate. This phenomenon is known as

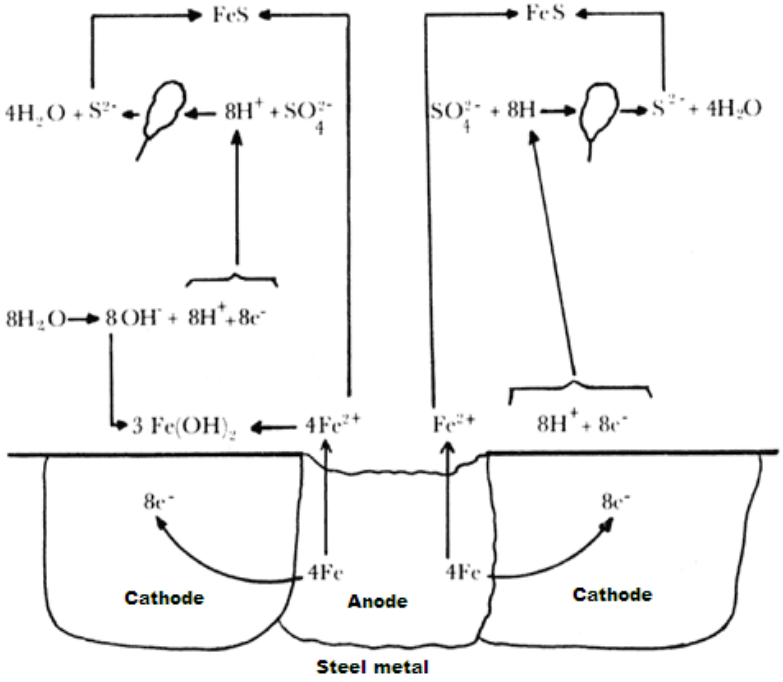

Figure 2: Schematic representing bacterial corrosion of iron by the *Desulfovibrio*. FeS is the corrosion product. The overall reaction: $4Fe + SO^{4-} + 4H_2O \rightarrow FeS + 3Fe(OH)_2 + 2OH$. (Iverson, 1968)

cathodic polarization which is when the potential of either the anode or the cathode, or both, is changed.

The impact of redox potential in determining metal solubility and transport is shown for copper (Figure 3). The normal pH of wáter in Bowling Green is around 8. Once the pH incrases to 10, copper binds to oxygen as seen in Figure 3 to form copper oxide (Garrels and Christ, 1965).

Malachite as a result of copper pipe corrosion

With the occurence of corrosion, malachite ($Cu_2 (OH)_2 CO_3$), a common copper mineral is formed. It is a copper carbonate hydroxide substance and is usually green in color. It is seen in fibrous structures. Malachite is formed by copper weathering over time and it is also seen with azurite ($Cu_3 (CO_3)_2 (OH)_2$) and calcite (Garrels and Christ, 1965**).**

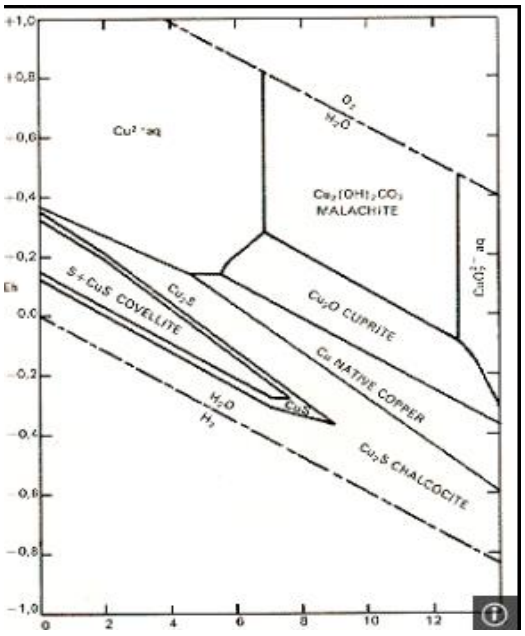

Figure 3: Eh-ph Diagram for Cu-H_2O-O_2-S-CO_2 System (Garrels and Christ, 1965**).**

Corrosion Problem in Bowling Green, Kentucky

Recently, corrosion of wáter pipes in Bowling Green, Kentucky has sharply increased. While age was the most common factor initially considered, most of these recent breaks have been in copper pipes less than 20 years old. Moreover, these pipes have corroded from the outside, rather than the inside. These breaks have occured in copper pipes within a few feet of a curb, under the roadway, leading to speculation as to the factors leading to the breaks, such as the bedding materials (limestone rocks and the constant vibrations from the roadway from the movement of traffic. Figure 4 shows the pipes were corroded from the outside. The original pipe retained most of its thickness and native material.

Figure 5 shows the trenching and bedding process used by the City of Bowling Green. The trench that is dug for the pipe is about 30 to 36 inches deep and is below the frost line. Ground limestone are used as the bedding material with a size designated as "nines" (passed through a number 9 sieve or "57's" passed through a number 57 sieve). The "57's" include finer bedding material and is dustier. Depending on the location in the country, other bedding materials may be used. For example, areas with fly ash available will use fly ash, which is known to increase the rate of corrosion. Recently, the copper pipe connection to the mainline changed through the use of a PVC connecter. There is now no direct contact of the copper metal with the main wáter line. Figure 5 illustrates the PVC and it shows that there is no direct contact (BGMU, 2007). The purpose of this thesis

is to examine the factors, particularly the bedding materials and vibrational motion, which could be contributing to the corrosión of copper wáter pipes in Bowling Green, Kentucky.

Figure 4: Corroded water pipe sample from Bowling Green, KY

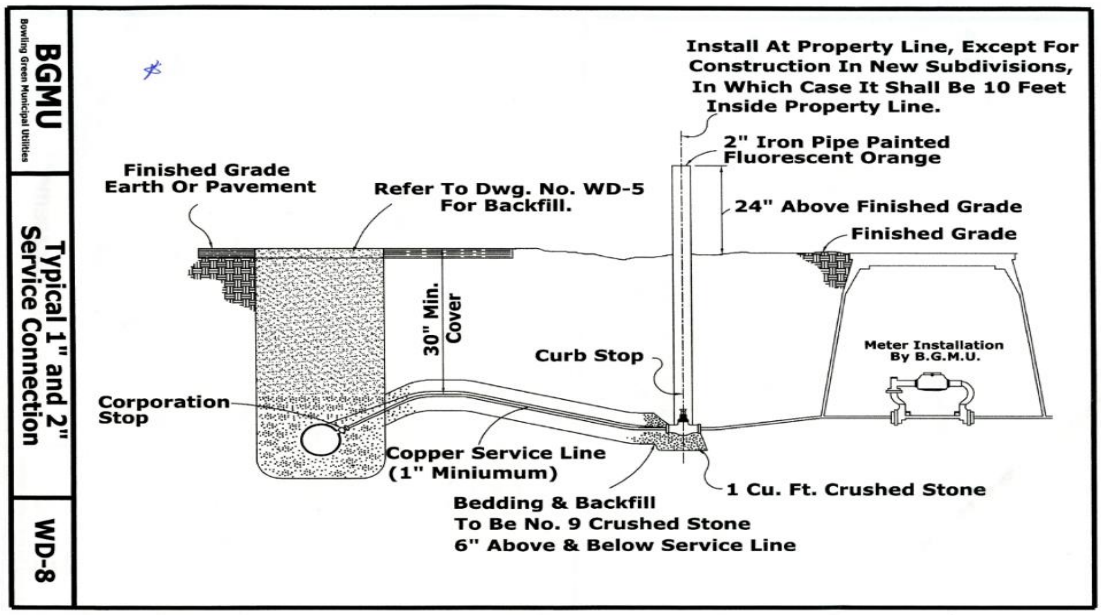

Figure 5: Profile of the bedding design used in Bowling Green Wáter and sewer systems (BGMU, 2007)

MATERIALS AND METHODS

This chapter describes the materials, methods, and experimental approaches used to examine the contributing factors for the recent corrosive failures of copper wáter pipes in Bowling Green, Kentucky. All of the copper pipe samples, corroded and uncorroded, and bedding materials used in this thesis were generously provided by Bowling Ggreen Municipal Utilities.

Materials

Ten corroded copper pipes have been randomly, labeled A to I. These pipe samples were from actual failures in Bowling Green. Table 2 provides the list of materials used.

Table 2: Materials used in experimental studies and sources.

Chemicals/ Materials	Company Obtained From
Nitric acid, Trace Metal Quality	EM Science
Water, D.I water	Department of Chemistry
Limestone "9s"	Bowling Green Municipal Utilities
Copper pipes labeled A to I	Bowling Green Municipal Utilities

Methods

Scanning Electron Microscopy (SEM): The scanning electron microscope (SEM) uses a focused beam of high-energy electrons to generate a variety of signals at the surface of solid specimens. It is also capable of performing analyses of selected point locations on the sample. Semi-quantitatively determining chemical compositions using EDS. Also, data are collected over a selected area of the surface of the sample. Figure 3 shows a typical SEM instrument, showing the electron column, sample chamber, EDS detector, electronics console, and visual display monitors (Susan Swap, 2004).

Figure 6: SEM and EDS (Susan Swap, 2004)

The pipe samples, which were randomly labeled A to I, were cut to small pieces. The sample was placed inside the sample chamber. The sample were fixed and not exposed to any movement until the image appeared clear. Pipe surface exteriors were compared with their interior. The SEM filament was set to 20 V. The corroded material on the outside of the pipes was removed and also viewed. SEM was used to obtain elemental composition and quantitative analysis.

X-ray Diffraction (XRD): X-ray crystallography is a technique that involves passing a beam of X-rays through a crystal substance. The beam is split into several directions due to the symmetry of the group of atoms and diffraction, resulting in a pattern of intensities which can be interpreted as the location of the atoms in the crystal, using Bragg's law. It is one of the primary techniques used to elucidate crystal structures, due to its precision and reliability.

Acid Digestion: Selected pipe samples were digested by acid and analyzed for copper.

Pipe C: A sample mass of 7.30 g was weighed. It was cut into pieces and put into a 250 ml beaker and then 25 ml of water and 25 ml of nitric acid was added. The solution was left for two hours to dissolve. The solution was transfered to 100 ml volometric flask and the volumen was made up to 100 ml with deionized wáter. The solution was transferred into a glass bottle and labelled.

Pipe F: A sample mass of 5.29 g was weighed. It was cut into pieces and put into a 250 ml beaker and then 25 ml of water and 25 ml of nitric acid was added. The solution was left for two hours to dissolve.. The solution was transfered to 100 ml volometric flask and the volumen was made up to 100 ml with deionized wáter. The solution was transferred into a glass bottle and labelled.

Pipe K: A sample mass of 8.11 g was weighed. It was cut into pieces and put into a 250 ml beaker and then 25 ml of water and 25 ml of nitric acid was added. The solution was left for two hours to dissolve. The solution was transfered to 100 ml volometric flask and the

volumen was made up to 100 ml with deionized wáter. The solution was transferred into a glass bottle and labelled.

Pipe J: A sample mass of approximate 7.20 g was weighed .It was cut into pieces and put into a 250 ml beaker and then 25 ml of water and 25 ml of nitric acid was added. The solution was left for twenty four hours to dissolve. The solution was transfered to 100 ml volometric flask and the volumen was made up to 100 ml with deionized wáter. The solution was transferred into a glass bottle and labelled.

New Pipe (NP): A sample mass of 4.11 g was weighed. It was cut into pieces and put into a 250 ml beaker and then 25 ml of water and 25 ml of nitric acid was added. The solution was left for twenty four hours to dissolve. The solution was transfered to 100 ml volometric flask and the volumen was made up to 100 ml with deionized wáter. The solution was transferred into a glass bottle and labelled.

Inductively coupled plasma optical emission spectroscopy (ICP-OES): This technique is used for elemental analysis for trace elements in mg. The ICP of the copper pipes of dilutions was prepare 5 µl of sample and diluted with 10% nitic acid to total volume of 50 ml or a one to ten thousand dilution because the sample was very concentrated. The final solutions were analyzed with no particulates in them. Usually the analyte concentration

range of is between 1 ppm to 500 ppm. The 1-500 ppm is a general ideal range for most elements for excellent results.

Potential limestone impacts on copper pipes

Limestone of different sizes (size 57 and 9) from BGMU was collected because these are used in pipe line bedding. Limestone "9's" was placed into 6 different flasks up to the 100 ml mark. A small piece of pipe was put into the flask and more limestone added up the 250 ml mark. Water was added and the flask was placed on a shaker.

The first flask had limestone with water and the pipe. The SEM image of the pipe was checked after 2, 4 and 6 weeks. The second flask had limestone, water, and the pipe. The SEM image of the pipe was checked after 4, 6 weeks. The third and fourth flasks had limestone, water, and the pipe for 6 weeks and the SEM image was checked after 6 weeks. The third flask was not put on the shaker while the fourth flask was. The fifth and sixth flasks had only limestone and the pipe for 6 weeks; the SEM images were checked after 6 weeks. This experiment was performed to see the effect limestone has on copper pipes, even after a short period of time, and to see if it enhances the corrosion of copper pipes under vibrational motion.

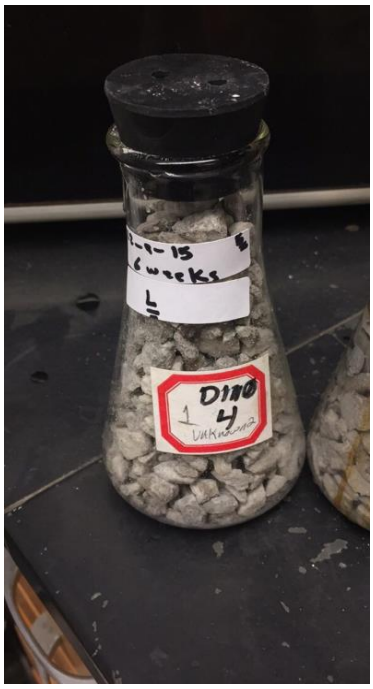

Figure 7: Flask containing limestone and pipe

RESULTS AND DISCUSSIONS

This chapter discusses the experimental results from Scanning Electron Microscopy (SEM) characterization of the corroded and uncorroded surfaces of the pipe materials, theX-ray diffraction (XRD) analysis of the minerals on the surfaces of the pipes, and the temporal studies that were used to examine the impact of the limestone bedding material and vibration on the surface of the pipes.

Figure 7 shows the SEM images of the inside and outside area of a new, uncorroded pipe. The SEM images of the new pipe inside area (Figure 7) indicate the surface is clean and smooth with only a very small amount of "islands" of impurities. On the smooth area, the data shows the surface is predominantly copper as expected [Cu (41.138%), Cl (0.369%), C (46.636%) and O (11.857%)] with slight impurities. Analysis of one of the "islands" shows Cu (7.125%), C (76.941%), O (14.865%), Si (0.108%), P (0.052%), S (0.207%), Cl (0.264%), K (0.276%) Ca (0.046%) and Fe (0.117%). SEM images from the same pipe, but on the outside (Figure 8) show a surface that is still relatively clean, but with a slight increase in impurities. Four spots for selected for elemental analysis – two from clean areas and two from impurities. The clean spots indicated predominantly copper with a few trace elements such as Na, Mg, Al, Si, Cl, K and Ca. The impurity areas, which are likely to be copper oxide, had higher levels of trace elements. There are more impurities on the outside and are likely to include Al_2O_3, SiO_2 and $CaCO_3$, which were not observed on the inside area. The brown boxes on the SEM images show the areas that were analyzed.

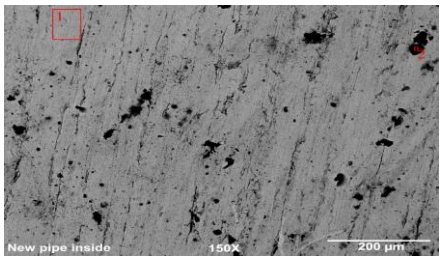

Atomic Percentage	Spot 1	Spot 2
C	46.636	76.941
O	11.857	14.865
Cl	0.369	0.264
Cu	41.138	7.125
Si	-	0.108
P	-	0.052
S	-	0.207
K	-	0.276
Ca	-	0.046
Fe	-	0.117
Total	100	100

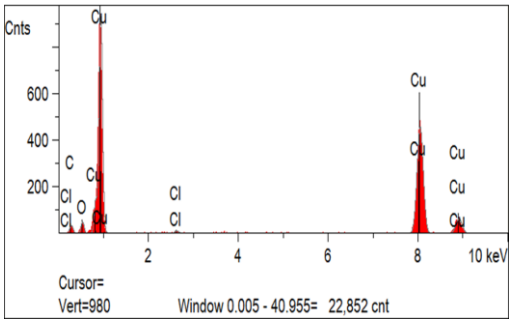

Figure 8: SEM image and analysis of the inside of a new copper pipe.

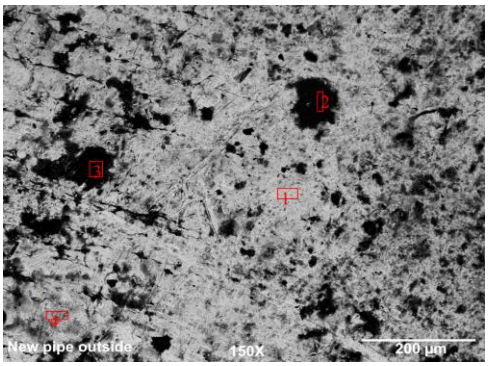

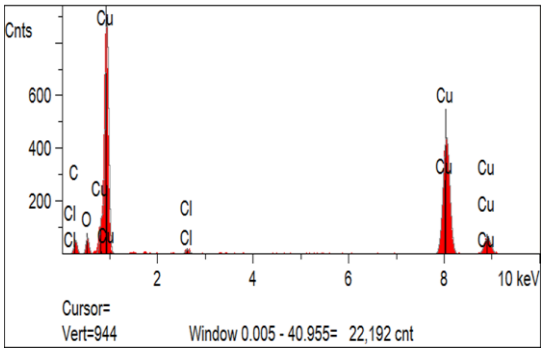

Atomic Percentage	Spot 1	Spot 2	Spot 3	Spot 4
C	52.612	21.712	56.013	55.500
O	13.294	41.216	31.710	21.032
Cl	0.489	-	0.475	0.808
Cu	33.605	4.682	0.577	19.737
Al	-	7.425	0.678	0.761
Si	-	9.025	1.991	0.919
K	-	0.636	0.375	0.126
Ca	-	0.292	4.447	0.221
Ti	-	1.565	-	-
Fe	-	1.337	0.450	-
Na	-	-	0.481	0.817
S	-	-	0.349	-
Mg	-	-	0.577	0.079
Total	100	100	100	100

Figure 9: SEM image and analysis of the outside of a new copper pipe

Figure 9 shows the SEM images of the inside area of corroded pipe C. The SEM images show flower-like growths which appear on the surface. Compositions were analyzed for three areas. Spot 1 is on the flower-like area, while spots 2 and 3 were taken on the smooth area. Spot 1 contains Cu (17.00%), Al (13.54%), Si (4.40%), Ca (0.55%) and O (64.51%). Spot 2, which is darker than spot 3, contains Cu (10.72%), Al (19.06%), Si (6.53%), Ca (0.67%), Cl (0.35%) and O (62.67%). Spot 3 contains Cu (27.57%), C (7.93%), O (48.34%), Si (3.87%) and Al (12.29%). From the data shown above, it is most likely that the flower-like material is CuO while spot 2 is where CuO is just starting to grow. Figure 10 is from the outside of corroded pipe C and shows the presence of copper minerals such as malachite and azurite or to other common minerals such as goethite, and calcite.

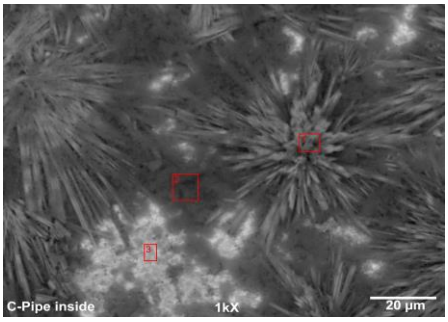

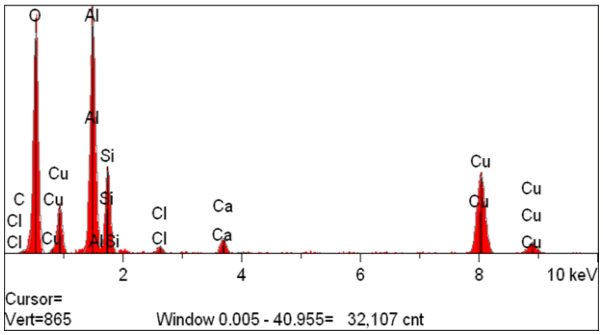

Atomic Percentage	Spot 1	Spot 2	Spot 3
C	-	-	7.93
O	64.51	62.67	48.34
Cl	-	0.35	
Cu	17.00	10.72	27.57
Al	13.54	19.06	12.29
Si	4.40	6.53	3.87
K	-	-	-
Ca	0.55	0.67	4.447
Total	100	100	100

Figure 10: SEM image and analysis of the inside of pipe C

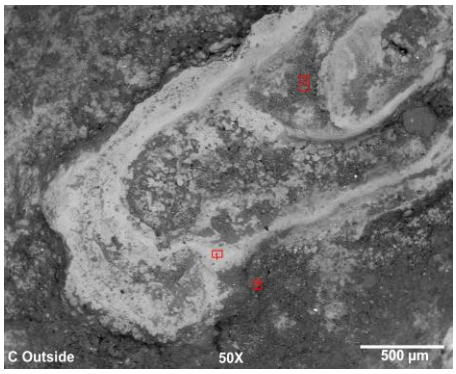

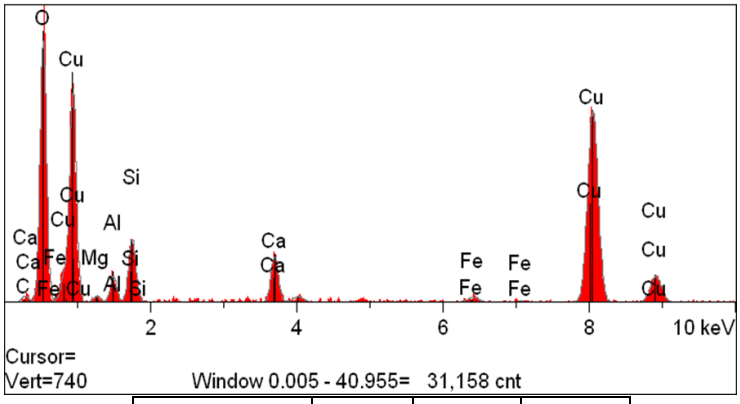

Atomic Percentage	Spot 1	Spot 2	Spot 3
C	7.76	8.52	-
O	62.11	70.78	58.29
Cl	-	-	-
Cu	21.04	4.682	18.82
Al	2.12	2.10	3.77
Si	4.17	4.26	10.24
K	-	0.17	0.50
Ca	1.59	9.56	5.87
Ti	-	-	-
Fe	0.36	0.39	-
Na	-	-	-
S	-	-	-
Mg	0.86	1.35	2.52
Total	100	100	100

Figure 11: SEM image and analysis of the outside of pipe C

Figure 11 shows a SEM image of the inside area of corroded pipe E. From the SEM image of the inside area, data were taken on four spots. Spot 1 is on the area with a lot of needle-like material. Spot 2 is the place with more small particles. Spot 3 is the darkest area, while spot 4 is the brightest. Spot 1 data are Cu (18.60%), Al (15.61%), Si (7.61%), Ca (0.62%), C (1.90%), Fe (0.29%) and O (55.33%). Spot 2 data are Cu (3.55%), Al (11.18%), Si (17.77%), Ca (0.37%), Fe (1.33%), Mg (0.61%), K (0.35%), Cl (0.09%) and O (65.04%). Spot 3 data are Cu (18.82%), O (50.79%), Al (18.36%), Si (10.88%), Ca (0.62%), Cl (0.16) and Fe (0.36) while Spot 4 showed Cu (15.35%), O (58.10%), Al (16.22%), Si (9.41%), Ca (0.62%) and Cl (0.30%). Spot 2 contains much more Si than the other areas, which means the small particles are likely SiO_2. Spot 3 and Spot 4 are similar. From the SEM image of the outside area (Figure 12), there are not big blocks like what is shown on inside surface. Compared to the inside area, the outside one is much smoother with more small particles on the surface. In the smooth area, the analysis shows Cu (50.13%), O (43.48%), Al (1.23%), Si (3.07%) and Ca (2.09%), while the small particles contain Cu (19.53%), Al (1.20%), Si (3.76%), Ca (4.77%), Fe (0.29%), Mg (1,10%), K (0.11%), C (22.74%) and O (46.51%). In comparison to the uncorroded pipe outside area,there are more impurities in the small particles on the surface and the amount of C is also larger.

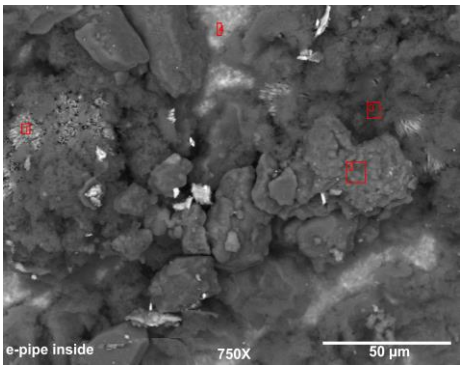

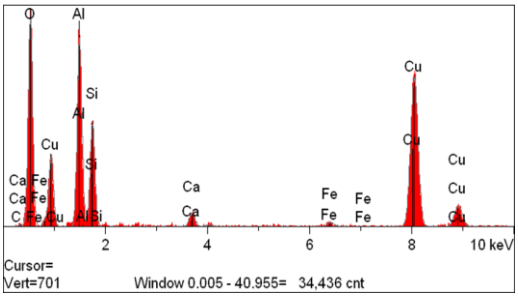

Atomic Percentage	Spot 1	Spot 2	Spot 3
C	7.76	1.90	3.55
O	50.79	55.33	65.04
Cl	0.16	-	0.09
Cu	18.82	18.60	18.82
Al	18.36	15.61	11.18
Si	10.88	7.64	17.77
K	-	-	0.35
Ca	0.62	0.62	0.37
Ti	-	-	-
Fe	0.36	0.29	1.03
Na	-	-	-
S	-	-	-
Mg	-	-	0.61
Total	100	100	100

Figure 12: SEM image and analysis of the inside of pipe E inside

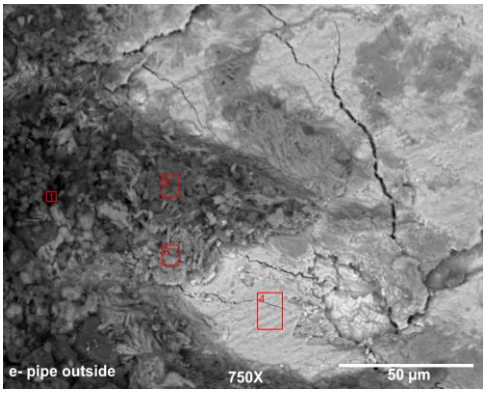

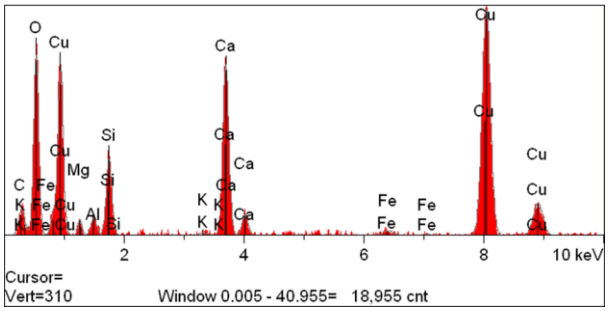

Atomic Percentage	Spot 1	Spot 2	Spot 3	Spot 4
C	22.74	1.90	3.55	
O	46.51	55.33	65.04	
Cl	0.16	-	0.09	
Cu	19.53	18.60	18.82	
Al	1.20	15.61	11.18	
Si	3.76	7.64	17.77	
K	0.11	-	0.35	
Ca	4.77	0.62	0.37	
Ti	-	-	-	
Fe	0.29	0.29	1.03	
Na	-	-	-	
S	-	-	-	
Mg	1.10	-	0.61	
Total	100	100	100	

Figure 13: SEM image and analysis of pipe E outside

Overall, the SEM analysis of all of the corroded pipes shows large increases in impurities versus the uncorroded pipe, particularly for the trace elements. Additionally, Inductively coupled plasma spectroscopic elemental analysis of bulk samples of all of the corroded and uncorroded pipes showed >99.9% copper, as expected.

XRD

X-ray diffraction measurements were taken to determine what minerals wee on pipe C's inside and outside surface. By matching the testing results to a data bank, the inside surface of the pipe contained silicon dioxide (SiO_2, Quartz), copper hydroxide carbonate ($Cu_2(OH)_2CO_3$, Malachite), calcium carbonate ($CaCO_3$) and copper oxide ($Cu_{2+1}O$, Cuprite, syn). The outside surface contains copper hydroxide carbonate ($Cu_2(OH)_2CO_3$, Malachite), iron aluminum oxide ($Fe_2Al_2O_4$, Hercynite, syn), calcium carbonate ($CaCO_3$, Calcite, syn), silicon oxide (SiO_2, quartz low) and copper oxide (Cu_2O, Cuprite).

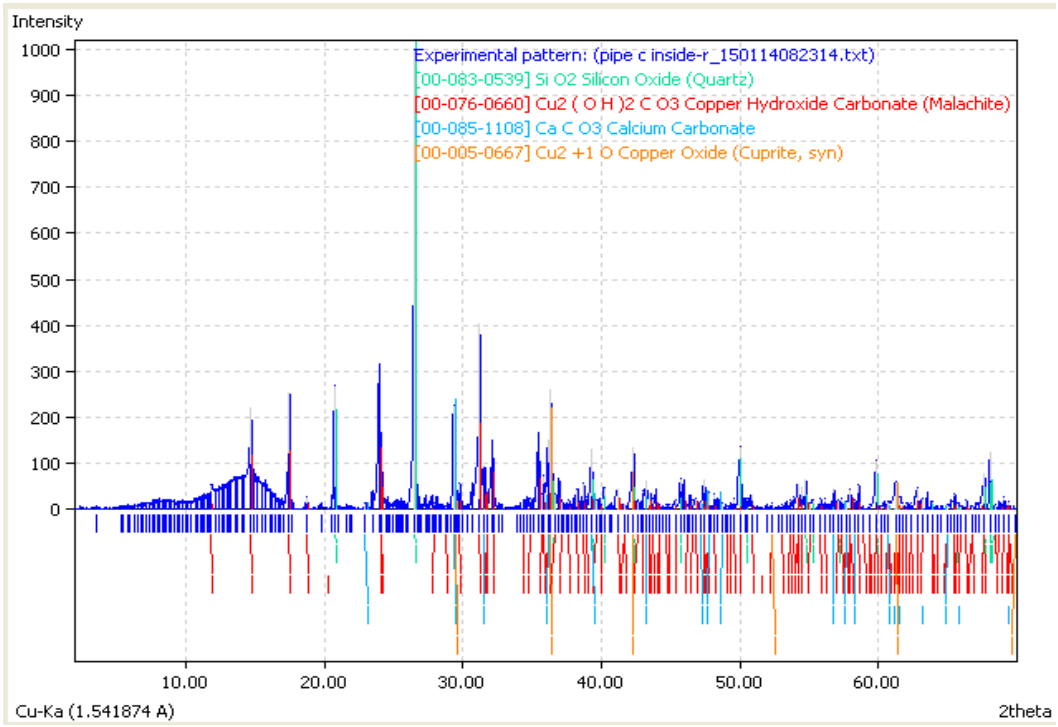

Figure14: XRD spectra of the poder inside of C copper pipe.

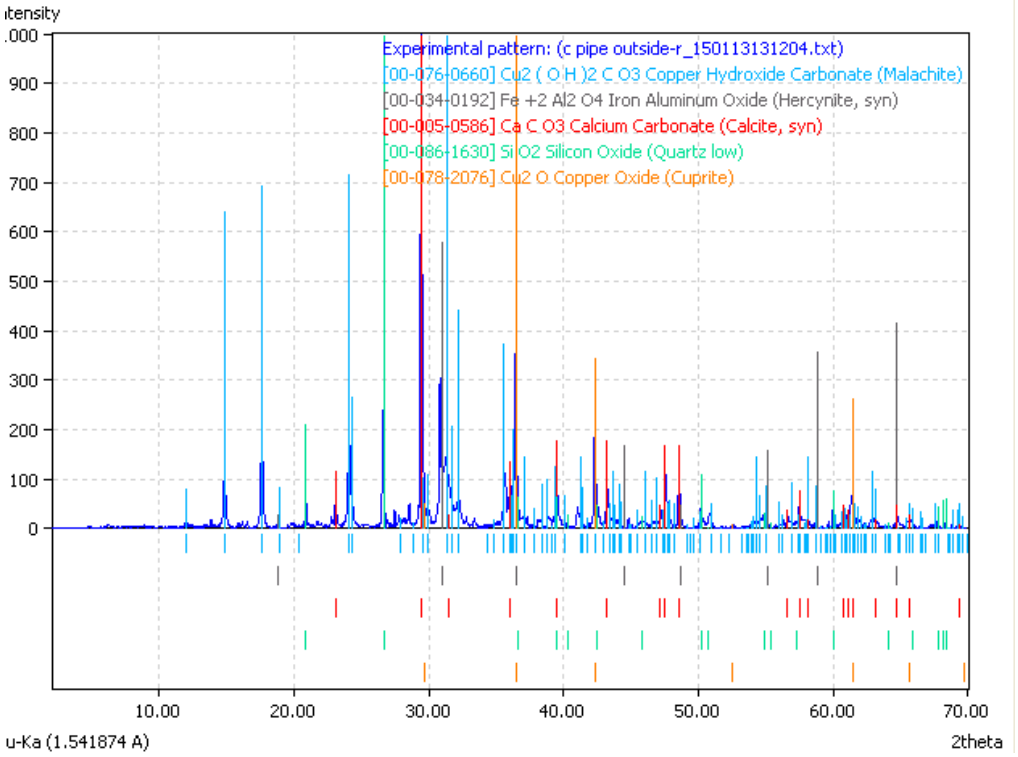

Figure 15: XRD spectra of the inside powder of corroded copper pipe.

Temporal Studies of Limestone on Copper

Limestone (size 9) from BGMU was placed into contact with a small flat piece of uncorroded copper pipe with a small x scratched onto the surface. The limestone, which is used as the bedding material in the ground, was placed into six different flasks up to the 100 ml mark. A small piece of pipe was put into the flask and more limestone added up to the 250 ml mark. Except where noted, all flasks were placed on a wrist shaker for 2, 4, and/or 6 weeks. The first flask had limestone with water and the pipe. The SEM image of the pipe was checked after 2, 4 and 6 weeks. The second flask had limestone, water, and the pipe. The SEM image of the pipe was checked after 4, 6 weeks. The third and fourth flasks had limestone, water, and the pipe for 6 weeks and the SEM image was checked after 6 weeks. The third flask was not put on the shaker. The fifth and sixth flasks had only limestone and the pipe for 6 weeks after which the SEM images were checked. The fifth flask was not put on the shaker. These experiments were performed to study the effect limestone has on copper pipes and to see if the corrosion of copper pipes is enhanced under vibrational motion.

New or uncorroded pipe with limestone after two weeks

Figure 15 shows the SEM image of uncorroded pipe with pipe in contact with water, limestone and vibrations was compared after two weeks of vibrations. After two weeks, the pipe showed longer sections of dark spots forming line-like structures. This could be due to the scraping of limestone on the pipe under the conditions of shaking.

The SEM analysis showed the percentage of calcium on the surface as did oxygen, showing that calcium carbonate is
depositing on the surface. A trace amount of iron deposits were also detected. The iron can be from either the water or limestone.

Atomic Percentage	Spot 1	Spot 2
O	51.882	52.084
Mg	3.530	1.936
Al	4.891	0.052
Si	9.832	0.558
Cl	1.066	0.062
Ca	15.076	10.872
Fe	1.035	0.263
Cu	12.688	5.068
O	-	29.106
Total	100	100

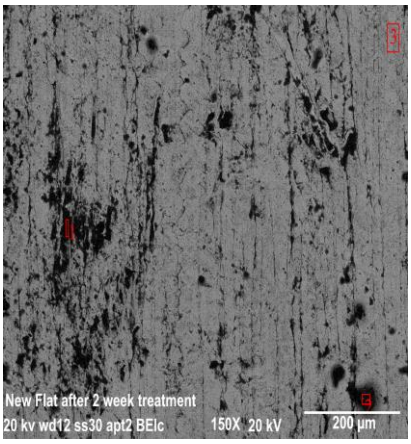

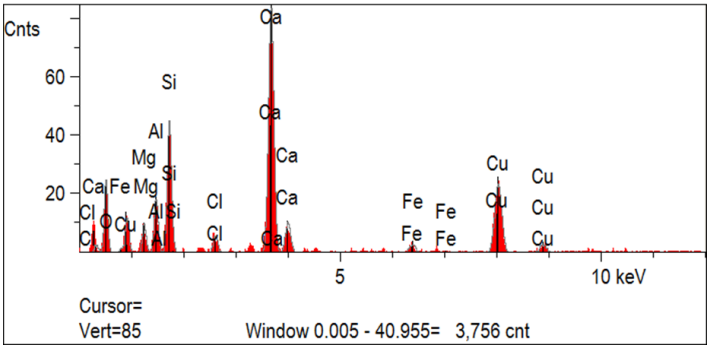

Figure 16: SEM image and analysis of new pipe and limestone after two weeks

Figure 16 shows the SEM image of new pipe and limestone after four weeks. From the SEM image, we can see a lot of black particles or spots and a two rod like structures. EDS data were taken on two spots. Spot one is on the area with clear Surface. Spot 2 is the place with more big black particles. The table shows the atomic percentage of the elements present in on the two spots.

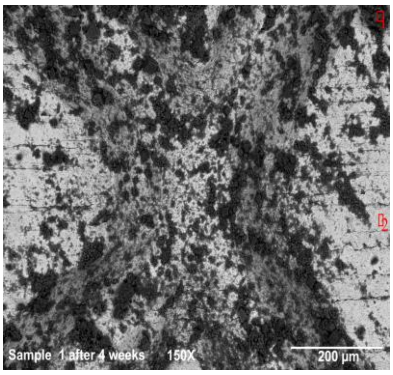

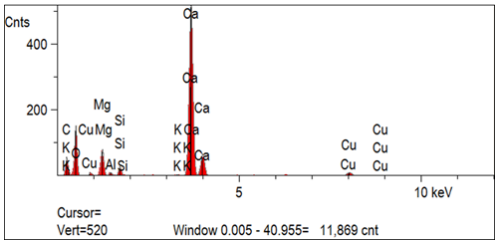

Atomic Percentage	Spot 1	Spot 2
C	23.766	25.262
O	58.221	11.075
Mg	3.151	-
Al	0.319	-
Si	0.685	-
K	0.058	-
Ca	12.955	-
Cu	0.846	63.662
Total	100	100

Figure 17: SEM image and analysis of new pipe and limestone after four weeks

Comparsion between two weeks and four weeks interaction with limestone

The percetage of oxygen is higher in the 4 weeks interaction than in the 2 weeks interaction. We also see the presence of copper which is from the limestone. The percentage of copper has also decreased in great value. The percentage of oxgyen has also increased.

Figure 17 shows the SEM image of flat clean copper pipe. The SEM image of the X scratch is very clean. SEM images between the two ends of the X scratch were also analyzed. While there are both spot and bright spots, the surface is generally very clean and smooth and contains mostly copper while the spots are probably mostly copper oxide.

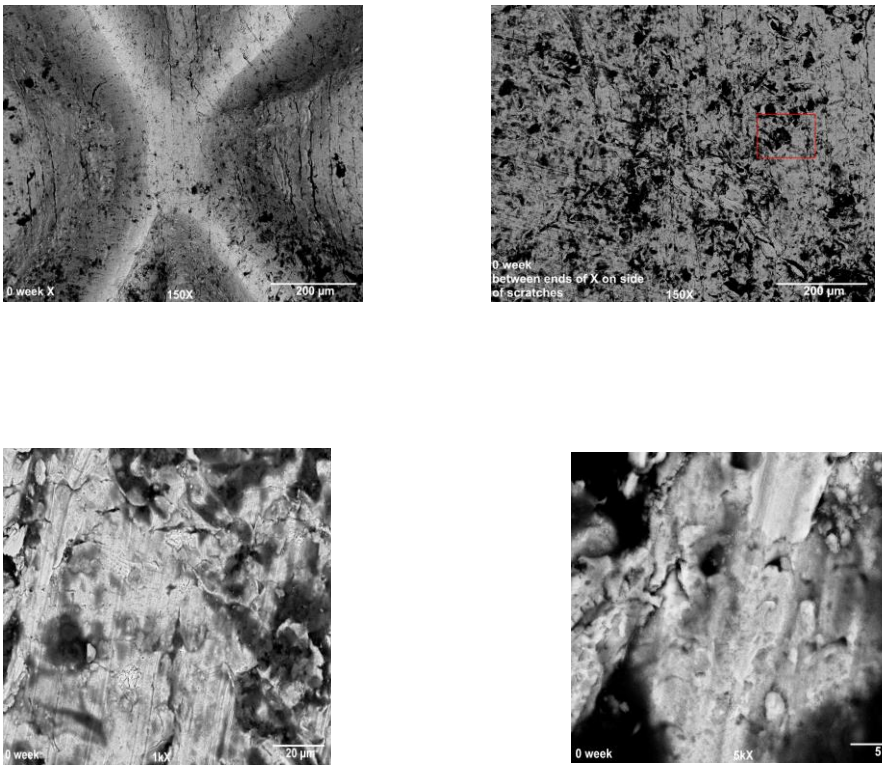

Figure 18: SEM image and analysis of flat clean coper pipe

Figure 18 shows the SEM image of flat copper pipes with water, limestone, and vibration after 6 weeks. The SEM images show many more impurities, which contains calcium and oxygen and are probably calcium carbonate deposits from the limestone. Moreover, expanded views of the surface shows substantial pitting, growths of calcium carbonate filling in the pits and growing together. The 5K image show a lot of pitting on the surface because limestone causes damage on the surface.

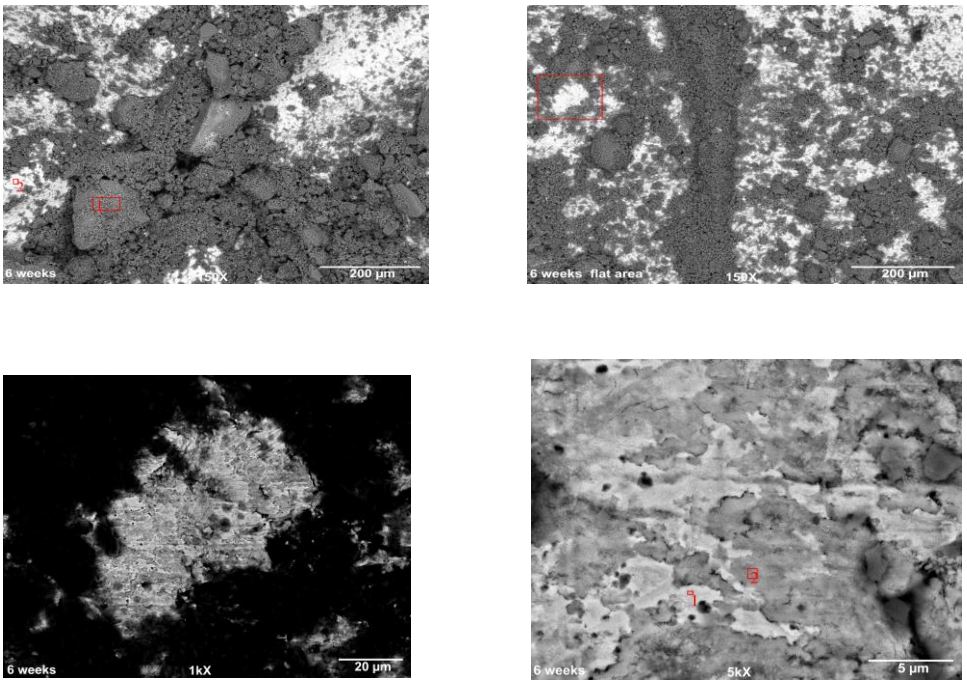

Figure 19: SEM image of flat copper pipes with water, limestone, and vibration after 6 weeks.

The effect of water is clear. Figure 19 shows SEM image of flat copper pipes with limestone, vibration, and no water after 6 weeks. Little pitting is observed. The X scratch is clean and clear. The dark areas are calcium carbonate but this appears to be mostly dust that settled onto the surface and grooves.

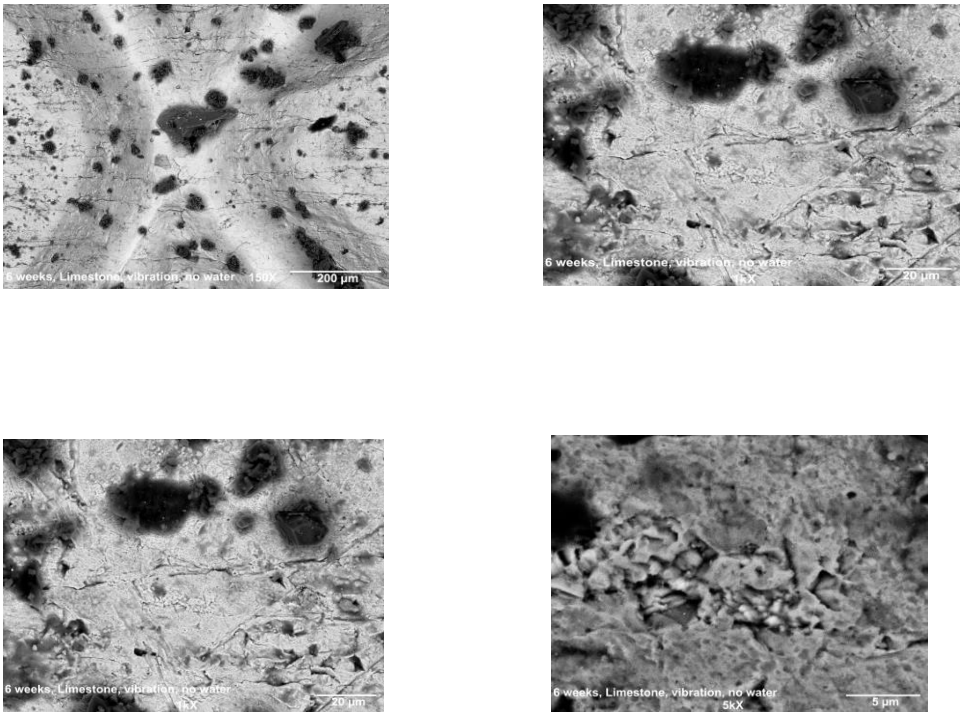

Figure 20: SEM image of flat copper pipe with limestone, vibration, and no water after 6 weeks.

Figure 20 shows the SEM image of flat copper pipe with limestone but with no water and no vibration. From SEM image of X scratches and flat area, we can find it has only slight impurities. The dark areas are calcium carbonate. This sample indicated what dust from the limestone on the surface would be, although even dust creates a slightly impacted surface

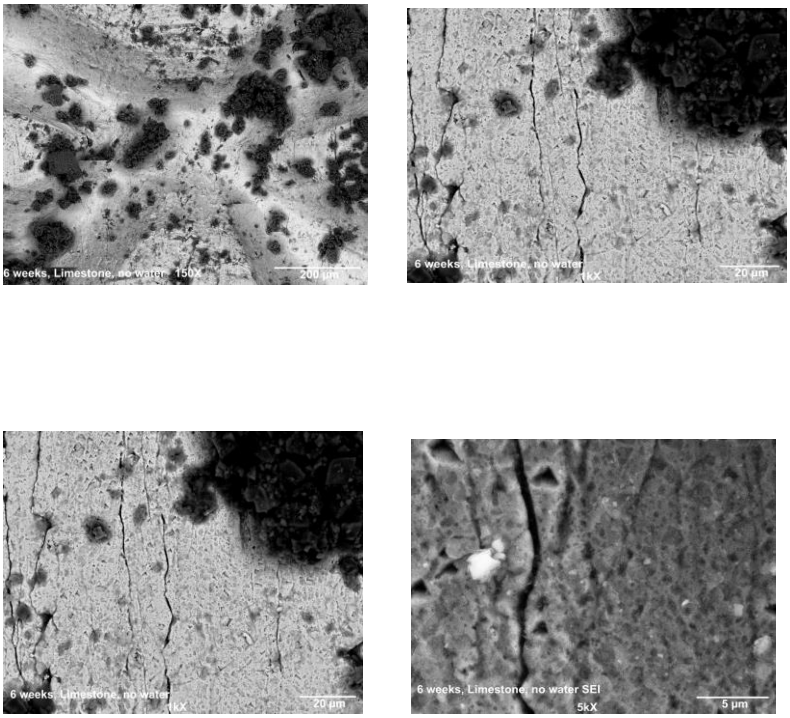

Figure 21: SEM image of flat copper pipe with limestone, no vibration, and no water after 6 weeks.

Figure 21 shows SEM image of flat copper pipe with limestone and water but no vibration. From the image of the X scratch and the flat area, we see increased pitting and calcium carbonate deposits. Even without vibration, the presence of water allows surface reactions to take place with the limestone. However, the vibrational motion clearly sharply enhances the deposition of calcium carbonate and changes in surface morphology.

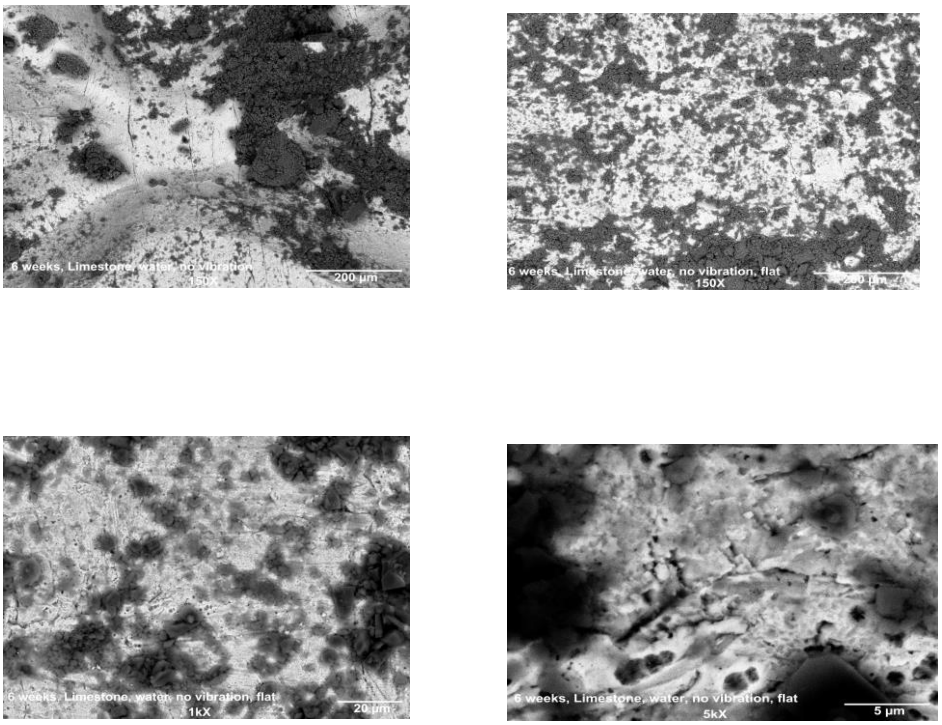

Figure 22: SEM image of flat copper pipe with limestone, water, and no vibration, after 6 weeks.

In conclusion, this straightforward experiment clearly shows that vibrational motion and water infiltration will enhance pitting and deposition of minerals on the copper surface. Over a period of 15-20 years, without the presence of a sacrificial anode, the progressive surface pitting could easily lead to pipe failures as seen by BGMU.

CONCLUSION

The increasing incidence of corroded copper water pipes in Bowling Green, Kentucky motivated the research of this thesis. The financial impact of premature pipe failures (occurring in 15 years, rather than the expected lifetime of 50 years) is more than $100,000 annually in Bowling Green which shows how important and timely the work is. It was critical to know if there was a pattern for the corrosion of copper pipes. Selected corroded copper pipes, provided by BGMU, were examined using methods such as scanning electron microscopy (SEM), energy-dispersive X-ray spectroscopy (EDS), X-ray diffraction (XRD) and inductively coupled plasma optical emission spectroscopy (ICP-OES). For the SEM studies, three corroded pipes were randomly selected from the varous pipes to examine the corroded surface as compared to uncorroded pipe.

The results from SEM analysis of shiny, new pipe had the a highest percentage of copper in the interior and exterior. The image showed a clean surface with few impurities.

Three corroded copper pipes were examined and their analysis was compared with new pipe. The SEM images of copper C its inside area, which was clean with some darker areas that is likely to be CuO. The outside area had many more trace elements and minerals including calcium carbonate and malachite. All of the corroded pipes had similar corroded outside surfaces and relatively clean, smooth inner surfaces.

The XRD analysis of pipe C confirmed the occurence of are copper hydroxide carbonate ($Cu_2(OH)_2CO_3$, Malachite), calcium carbonate ($CaCO_3$) both in the inside and outside, although mostly on the outside. Malachite is intensely green and can be seen visually on the outside.

The six week temporal studies confirmed that limestone in the presence of wáter and vibrational motion, such as under a roadway, near a curb, can cause measurable surface changes with increasing deposition of calcium carbonate. Given that the surface pH of calcium carbonate is near 10, the unexpectedly early failures, may require a change in how bedding is designed in these áreas. This study is focused on understanding the possible factors that may increase the rate of corrosión and it may also facilitate developments of methods to reduce copper pipe corrosión. Development of such methods will help reduce the amount of money spent on replacing copper pipes each year

FUTURE STUDIES

The SEM analysis of copper pipes over months of exposure to vibration and wáter should be examined as well as the impact of the presence of other trace analytes on the surface damage. This may allow the quantitative measure of the surface pitting.

PERSPECTIVE

It is important to note that there are no particular conditions or factors that cause corrosion. Although bacteria can create an environment for corrosion to occur by providing organic matter, there are many factors that aid the process.

Microscope images show patterns that provide understanding as to how the surface becomes pitted and damaged so that ways to prevent corrosión can be developed. Two important factors that clearly enhance the surface damages are the presence of wáter and vibrational motion. Initially, the limestone bedding was thought to prevent physical stress with no other impacts on copper. However, in our experiments where we had limestone in contact with wáter and new copper under vibrational motions, significant surface damage occurs in just 6 weeks.

REFERENCES

1. Sennour, M.; Marchetti, L.; Martin, F.; Perrin, S.; Molins, R. A detailed TEM and SEM study of Ni-base alloys oxide scales formed in primary conditions of pressurized water reactor. *Journal of Nuclear Materials*: Elsevier. **2010**, 402 (2-3), 147-156
2. Burleigh, T.; Gierke, C.; Fredj, N.; Boston, P. Copper Tube Pitting in Santa Fe Municipal Water Caused by Microbial Induced Corrosion. *Materials* **2014**, *7*, 4321-4334.
3. Mukhopadhyay, S. Sample preparation for Microscopic and Spectroscopic Charactrerization of Solid Surfaces and Films. *Department of Mechanical and Materials Engineering, Wright State University*: Dayton, Ohio. **2003**, 1-36.
4. Hamilton, W . Sulphate-Reducing Bacteria and Anaerobic Corrosion. *Annual Review of Microbiology*. **1985**, 39, 195-217.
5. Iverson, W. Microbial Corrosion of Metals. *Advances in Applied Microbiology*. **1987**, 32, 1–36.
6. Nawrockia, J.; Raczyk, U.; Świetlika, J.; Olejnikb, A.; Srokab, J. Corrosion in a distribution system: Steady water and its composition. *Water Research* **2010**, 4(6), 1863–1872.
7. Lytle, D.; Payne, J.; Schock, M. Corrosion Deposits. *U.S. Environment Protection Agency*: Cicinnati,Ohio. **2004**.
8. Bengough, D. G.; May, R. Seventh Report to the Corrosion Research Committee of the Institute of Metals. *The Journal of the Institute of Metals*. **1924**, 90-269.

9. Marshall, B. J. *Initiation, Propagation, and Mitigation of Aluminum and Chlorine Induced Pitting Corrosion.* Thesis, University of Virginia. **2004.**
10. Murray-Ramos, N. *Examining Aspects of Copper and Brass Corrosion in Drinking.* Thesis, University of Virginia. **2006**.
11. Lattyak, R. M. "Non-Uniform Copper Corrosion in Potable Water: Theory and Practice. Thesis, University of Virginia. **2007**.
12. Srivastava, A.; Balasubramaniam, R. Electrochemical impedance spectroscopy study of surface films formed on copper in aqueous environments. *Materials and Corrosion*. **2005**, 611-618.
13. Cong, H.; Michels, H.; Scully, J. R. Passivity and Pit Stability Behavior of Copper as a Function of Selected Water Chemistry Variables. *ECS - The Electrochemical Society*. **2009**, 141-164.
14. Coyne, J. *Flow Induced Failures of Copper Drinking Water Tube.* Thesis, University of Virginia. **2009**.
15. Rushing, J.C. *Advancing the Understanding of Water Distribution System Corrosion: Effects of Chlorine and Aluminum on Copper Pitting, Temperature Gradients on Copper Corrosion, and Silica on Iron Release.* Thesis, University of Virginia. **2002**.
16. American Water Works Association. *Internal Corrosion of Water Distribution Systems.* American Water Works Association. **1996.**

17. Marshall, B. *"Initiation, Propagation, and Mitigation of Aluminum and Chlorine Induced Pitting Corrosion.* Thesis, University of Virginia. **2004**.

18. Stansbury, E.; Buchanan, R. A. *Fundamentals of Electrochemical Corrosion.* ASM International. **2000**.

19. Nawrockia, Jacek; Raczyk-Stanisławiaka, Urszula; Świetlika, Joanna; Olejnikb, Anna & Srokab, Mirosława J. (**2012**). Corrosion in a distribution system: Steady water and its composition. Water Research Volume 44, Issue 6, March 2010, 1863–1872. http://www.sciencedirect.com/science/article/pii/S004313540900832X.

20. Warren, B.E.. X-Ray Diffraction (**1990**). 1st edition.

21. Water and sewer system improvements specifications for BGMU: Bowling Green, KY. January **2007**, 1-30.